

## ION MOTION IN THE ADIABATIC FOCUSER

E. Henestroza, A.M. Sessler, S. S. Yu, LBNL, Berkeley, California, U.S.A.\*

### Abstract

In this paper we numerically study the effect of ion motion in an adiabatic focuser, motivated by a recent suggestion that ion motion in an adiabatic focuser might be significant and even preclude operation of the focuser as previously envisioned. It is shown that despite ion motion the adiabatic focuser should work as well as originally envisioned.

### INTRODUCTION

The adiabatic focuser [1] works by having a focusing channel whose strength increases with distance down the channel. In this situation, electrons of various energies and various transverse oscillation phase all are transversely focused. The concept works with external focusing, but would be very effective in a plasma ion-focusing channel where the density of ions is simply increased as one goes down the channel. In the original work [1] motion of the ions was not included (as it was assumed to be a small effect).

Recently, it has been suggested that ion motion in an adiabatic focuser might be significant and possibly preclude operation of the focuser as previously envisioned [2]. In order to respond to this concern, in this paper we remove the previously made assumption that the ions do not move and numerically study ion motion in the adiabatic focuser. The ions clearly influence each other and, most importantly, are influenced by the electric field of the electrons being focused. However, taking parameters as originally developed, it is shown that, despite ion motion, the adiabatic focuser works as well as originally envisioned.

In the following we first (Section II) review the few equations that characterize the adiabatic focuser. This brief review serves to define the notation used in this paper. In Section III we describe the computational model employed, and in Section IV the results of the numerical studies are presented.

### ADIABATIC FOCUSER

In Ref. 1, the adiabatic focuser is developed using a 1D analysis appropriate, for example, to a flat beam. Although the numerical analysis in this paper is 3D, we follow the previous analysis, which is adequate to define terms. Let  $y$  be the transverse coordinate and  $s$  the distance along which the beam travels. The equation of motion is

$$\frac{d^2y}{ds^2} + K(s)y = 0, \tag{1}$$

with solution

$$y(s) = \beta^{1/2}(s) \cos[\psi(s) + \varphi], \tag{2}$$

where

$$\frac{d\beta}{ds} = -2\alpha(s), \tag{3}$$

and

$$\psi(s) = \int \frac{ds'}{\beta(s')}. \tag{4}$$

For simplicity we take  $\frac{d\beta}{ds}$  constant and, hence,

$$\beta(s) = \beta_0 - 2\alpha_0 s, \tag{5}$$

where  $\beta_0$  is the initial value of  $\beta$  while  $\alpha_0$  is the initial condition (and a constant throughout the focuser) and a measure of the degree of adiabaticity of the focuser.

The strength of the channel is readily determined as

$$K(s) = \frac{1 + \alpha_0^2}{\beta(s)^2} = \frac{1 + \alpha_0^2}{(\beta_0 - 2\alpha_0 s)^2}. \tag{6}$$

If we make the focusing channel from a plasma, this formula tells us how to vary the ion density from its initial value of  $n_0$  to its final value, obtained in length  $L$ , of  $n^*$ .

The high-energy beam is characterized by its energy  $E_0$ , its normalized emittance  $\epsilon_n$  and spot size  $\sigma (= \sqrt{\beta\epsilon})$  where  $\epsilon$  is the true emittance, i.e.,  $\epsilon_n/\gamma$ . The initial beam spot size is  $\sigma_0$  and the final spot size is  $\sigma^*$ .

### COMPUTATIONAL MODEL

The numerical studies were carried out using the code WARP [3]. The code was used to study the motion of the high-energy electrons and the ions. The low-energy electrons (resulting from the ionization process) were not included in the calculation. Although WARP is capable, in principle, of calculating the beam dynamics, including both the secondary (slow) electrons and the ions, we adopt for this paper a simple approximation based on ion motion alone. The approximation is based on the physical observation that secondary electrons are instantly expelled with the entry of the high-energy electron bunch. This secondary electron ‘‘clearing’’ will take place at any radial position as long as the charge of the ions enclosed is less than the charge of the high-energy beam. The secondary electrons will ‘‘pile up’’ at a radial position

\* Work supported by the U.S. Department of Energy, Office of Basic Energy Sciences, under Contract No. DE-AC02-05CH11231

where the net charge enclosed is zero. In the “underdense” regime considered in this paper, the secondary-electron pile-up will take place outside of the high-energy bunch. By Gauss’ Law, the secondary electrons will exert no force on the high-energy bunch, and can be ignored. The ions can then be modelled by a “bare” column with ion charge equal in magnitude to the charge of the high-energy bunch.

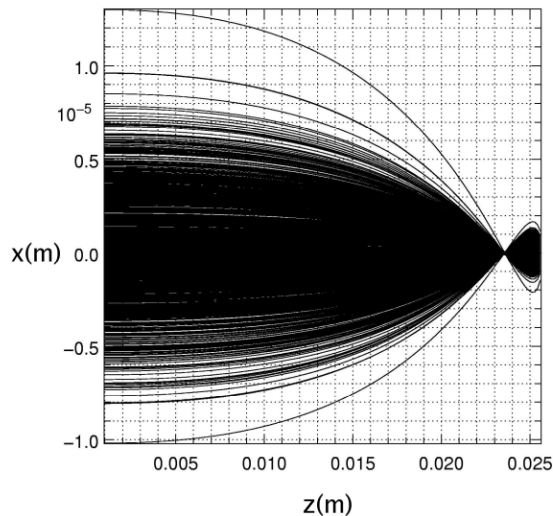


Figure 1: Electron trajectories with the ions fixed, and the high-energy electron bunch having zero emittance. The ions supply a focusing force as prescribed by Eq. 6.

The focuser works by first establishing a focusing channel of increasing strength, probably by means of differential pumping and then firing in an ionizing electron beam. The resulting plasma of low-energy electrons and ions remains (almost) fixed as it is electrically neutral. Then, subsequently, the high-energy pulse of electrons is fired into the plasma

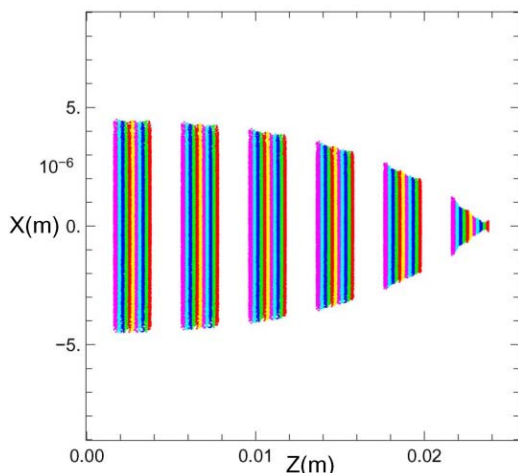


Figure 2: Snap shots taken as the high-energy electron bunch moves through the adiabatic lens focuser. The ions are allowed to move, and the high-energy electron bunch has zero emittance.

To model this system without including the low-energy electrons, we adopt the following method. First a distribution of “potential” ions is constructed with increasing density down the channel according to the prescription of the adiabatic focuser. Then, as the high-energy electrons enter the plasma they instantly create ions distributed radially over a region such that the ions in that region are equal to the number of electrons. Since the electron density is always higher than the ion density, one appreciates that the low-energy electrons are pushed out by the high-energy electrons until charge neutrality is obtained, i.e., over a larger radial region than the electron beam. This process is then repeated at each step. Once the ions are “created” they are free to move. (They don’t move prior to the high-energy beam entering the plasma due to the presence of the low-energy electrons.)

## RESULTS

The results of the numerical studies are presented in the figures. In the numerical computation we employed the parameters exhibited in Table I. At first we considered an “ideal adiabatic lens”, that is, one where the ions are in fixed locations and the high energy electrons have zero emittance. The result is shown in Fig. 1 and will provide a basis for comparisons with the more complicated cases next studied.

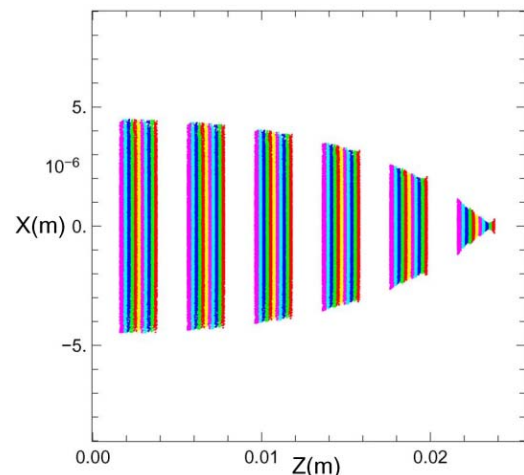


Figure 3: Snap shots taken as the high-energy electron bunch moves through the adiabatic lens focuser. The ions are allowed to move, and the high-energy electron bunch has non-zero emittance.

The first new result, namely, one in which the ions are allowed to move, is presented in Fig. 2. The electron beam is taken to have zero emittance so that a comparison with our base case (Fig. 1) can readily be made. In Fig. 3 we give the electron beam non-zero emittance and, once again, the focuser is seen to be as effective with ion motion included as it was when we assumed the ions were fixed. At the electron beam head, the ions have no time to move, and the beam envelope is therefore identical to the

frozen-ion case. Subsequent electron-beam slices see increasingly more ion bunching. Both the ion number as well as the radial distribution will change with time at a fixed axial location. However, a given electron slice will see an adiabatically varying ion distribution (with  $z$ ), and the concept of adiabatic focusing will continue to be effective.

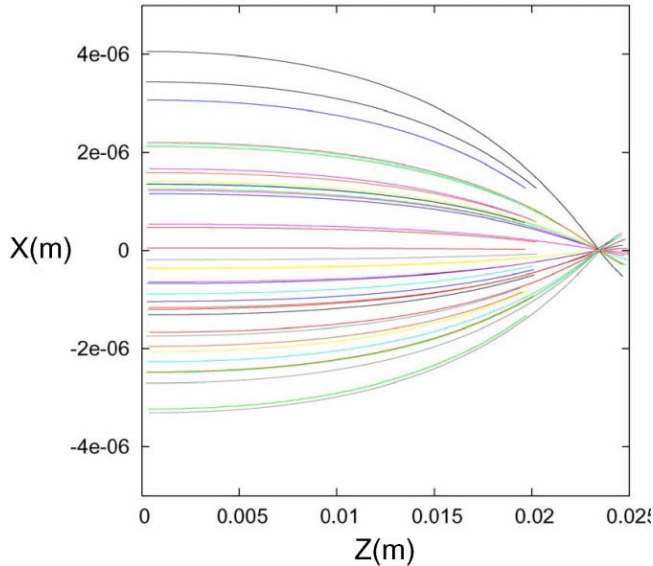


Figure 4: A few typical electron trajectories in the adiabatic focuser are shown.

Table 1: Parameters of the adiabatic focuser studied numerically

Initial Beam Parameters	
$E_0$ (GeV)	50
$\ell$ (mm)	1
$\epsilon_n$ ( $\pi$ -m-rad)	$3 \times 10^{-5}$
$\sigma_0$ ( $\mu$ m)	3
$\beta_0$ (cm)	3
Focuser Properties	
$\alpha_0$	$1/\sqrt{3}$
L (cm)	2.6
$n_0$ ( $\text{cm}^{-3}$ )	$8.4 \times 10^{15}$
$n^*$ ( $\text{cm}^{-3}$ )	$8.4 \times 10^{19}$
Final Beam Property	
$\sigma^*$ ( $\mu$ m) No ion motion	0.3
$\sigma^*$ ( $\mu$ m) With ion motion	0.3

Finally, in Figs. 4 and 5 we present some typical trajectories so that the reader can see, in detail, the strong focusing of electrons and the modest (inward) motion of the ions.

### CONCLUSIONS

The numerical studies were carried out only for the adiabatic focuser whose parameters are exhibited in Table I. It is clear however, since the high-energy electrons simply focus the ions even more than if they are held fixed, and reflecting upon how the adiabatic focuser “works”, it is evident that the general conclusion that ion motion will not preclude the effective operation of an adiabatic focuser, is true in general. We should also note that the ion motion can be reduced by going to heavier gases, as long as the electron-beam scattering effects are insignificant.

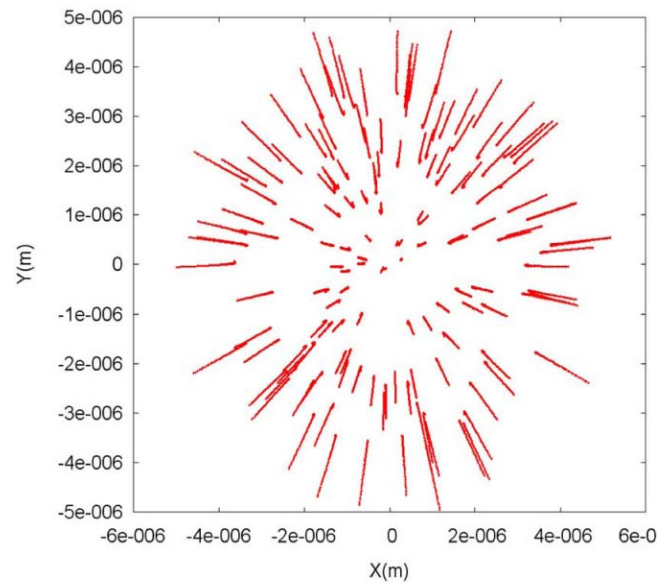


Figure 5: A few typical ion trajectories, at a fixed  $z$  location, in the adiabatic focuser are shown. One can see how the ions are first pulled in (focused) by the high-energy electrons and then blown up after the bunch passes by.

### REFERENCES

- [1] P. Chen, K.Oide, A.M. Sessler, and S.S.Yu, Phys. Rev. Lett. **64**, 1231 (1990).
- [2] J.R. Rosenzweig, et al, Phys. Rev. Lett. **95**, 195002 (2005).
- [3] D.P. Grote, A. Friedman, I. Haber, and S.S. Yu, Fusion Eng. Design **32-33**, 133 (1996).